

# IMPEDANCES OF BELLOWS CORRUGATIONS

King-Yuen Ng

*Fermi National Accelerator Laboratory, Batavia, IL 60510*

## **Abstract**

The longitudinal and transverse impedances of the bellows corrugations are analyzed systematically. Formulae are given so that, in the study of instabilities and energy losses, the impedances can be computed without resort to running a time consuming code like TBCI. The effect of many corrugations versus one corrugation is discussed.

## I. INTRODUCTION

Bellows form an indispensable part of the vacuum chamber in a storage ring. Their corrugations contribute significantly to the longitudinal and transverse coupling impedances which will lead to various types of instabilities as well as parasitic heating of the beam pipe. Although these impedances can be obtained by computing the wake potentials using the code<sup>[1]</sup> TBCI and then taking the Fourier transforms, the results are sometimes difficult to understand. The picture is usually further complicated by computation error due to the limitation of the finite mesh size and the truncation of the wake potential. It would be nice, if the coupling impedances can be estimated by formulae so that the instabilities can be discussed without the actual solving the Maxwell's equations numerically.

There are essentially two types of bellows systems: inner bellows and outer bellows. The outer bellows system is used, for example, in the Fermilab Main Ring. It consists of a pill-box cavity with a radius of roughly two times the beam pipe radius and some bellows corrugations. In the Fermilab Main Ring, the length of this cavity is about 15 cm and there are only about four to five bellows corrugations occupying about a tenth of the length. For this type of bellows system, the fields resonating in the pill-box cavity will dominate the fields in the corrugations. As a result, for impedance estimation, we can neglect the corrugations and study the cavity only. Below cutoff frequency, the impedances can be estimated by closing the cavity as if there were no beam pipes on both sides. Such a problem can then be solved exactly. The results are some sharp resonances. Above cutoff, fields leak away giving negligible contribution to the impedances. In many situations, these sharp resonances can be avoided by shielding the pill-box cavity by sliding shields at a radius approximately equal to the beam pipe radius. Such a bellows will then appear the beam particles as one or two very shallow pill boxes. The contributions to the impedances are then merely the small steps which are formula computable.

The inner bellows system consists of just corrugations of radius equal to that of the beam pipe. Therefore, the corrugations become the only contribution to the impedances. At low frequencies, the longitudinal and transverse impedances resemble the contribution of a step. At higher frequencies, a broad resonance is usually seen above cutoff. Such an impedance picture is more difficult to understand, and this paper will be devoted mainly to the discussion of the inner bellows.

If the picture of a broad resonance is assumed, the longitudinal coupling impedance can be characterized by three parameters: the resonant angular frequency

$\omega_r$ , the shunt impedance  $R_{\parallel}$  and the quality factor  $Q$ ; *i.e.*,

$$Z_{\parallel}(\omega) = \frac{R_{\parallel}}{1 - jQ \left( \frac{\omega_r}{\omega} - \frac{\omega}{\omega_r} \right)}. \quad (1.1)$$

Such an expression satisfies  $Z_{\parallel}(\omega) = Z_{\parallel}^*(-\omega)$  and is therefore a valid description of the longitudinal impedance. The transverse impedance, on the other hand, can be characterized by three similar parameters: the resonant angular frequency  $\omega_r$ , the shunt impedance  $R_{\perp}$  and the quality factor  $Q$ ; *i.e.*,

$$Z_{\perp}(\omega) = \frac{\omega}{\omega_r} \frac{R_{\perp}}{1 - jQ \left( \frac{\omega_r}{\omega} - \frac{\omega}{\omega_r} \right)}, \quad (1.2)$$

which is also a valid description of the transverse impedance because it satisfies  $Z_{\perp}(\omega) = -Z_{\perp}^*(-\omega)$  as well as

$$\int_{-\infty}^{\infty} Z_{\perp}(\omega) d\omega = 0. \quad (1.3)$$

As we shall see, both the position of resonance and  $R_{\parallel}/Q$  (or  $R_{\perp}/Q$ ) can be computed without TBCI. A rough estimate of  $Q$  can also be made.

In Section II, we shall study the impedance of a single corrugation hoping to get some insight into the general shape of the impedance. The position of the broad resonance  $\omega_r$  is then determined by solving an equation. An empirical formula is also given. In Section III, the low frequency behaviors of the impedances are discussed and the formulae for their computation are given. These quantities determine single-bunch mode-coupling instability growth rates and coupled-bunch instability growth rates. Then, the ratio of shunt impedance to quality factor can be inferred for both impedances. In Section IV, the loss factors are derived. In Section V, the effects of many corrugations versus one are discussed.

## II. ONE CORRUGATION

Let us begin by examining one *rectangular* corrugation of the bellows. Let  $b$  be the radius of the beam pipe,  $\Delta$  and  $2g$  be the depth and width of the corrugation respectively. Henke<sup>[2]</sup> has studied the problem in the frequency domain, which involves the solution of an infinite matrix equation. This complicated equation can be simplified tremendously<sup>[3]</sup> when  $g/b \ll 1$ . For clarity, only the result is quoted. The details can be obtained by following the derivation of Henke but retaining only

one term in the expansion inside the corrugation. The longitudinal impedance of such a rectangular corrugation as a function of frequency  $\omega/2\pi$  is

$$Z_{\parallel}(\omega) = \frac{gZ_0}{\pi b I_0^2(\bar{b}) D}, \quad (2.1)$$

where

$$D = j \frac{R'_0(kb)}{R_0(kb)} - 2kj \left[ \sum_{s=1}^S \frac{1}{\beta_s^2} \left( 1 - e^{-j\beta_s g} \frac{\sin \beta_s g}{\beta_s g} \right) - \sum_{s=S+1}^{\infty} \frac{1}{\alpha_s^2} \left( 1 - e^{-\alpha_s g} \frac{\sinh \alpha_s g}{\alpha_s g} \right) \right]. \quad (2.2)$$

In the above,  $k = \omega/c$ ,  $Z_0 = 377 \Omega$ ,  $I_0$  is the modified Bessel function of order zero,  $\bar{b} = bk/\gamma\beta$ ,  $\gamma$  and  $\beta$  are the relativistic velocity parameters of the beam particles. In the summations,  $\beta_s = \sqrt{(k^2 b^2 - j_{0s}^2)}$  and  $\alpha_s = \sqrt{(j_{0s}^2 - k^2 b^2)}$ , where  $j_{0s}$  is the  $s$ -th zero of the Bessel function  $J_0$  and  $j_{0S}$  is the zero that is just larger or equal to  $kb$ . Also,  $R(kb) = J_0(kb)N_0(kd) - J_0(kd)N_0(kb)$ , where  $d = b + \Delta$  and  $J_0$  and  $N_0$  are, respectively, the Bessel function and Neumann function of order zero. To have a deeper insight, let us take the limit  $kb \gg 1$  and  $g/b \rightarrow 0$ , then, by expanding the sine, sinh and the exponentials,  $D$  can be simplified to

$$D = -j \cot k\Delta + 2kg \left( \sum_{s=1}^S \frac{1}{\sqrt{k^2 b^2 - j_{0s}^2}} + \sum_{s=S+1}^{\infty} \frac{j}{\sqrt{j_{0s}^2 - k^2 b^2}} \right). \quad (2.3)$$

Here, in reality, the second summation cannot go to infinity because the expansion will break down as soon as  $\alpha_s g \simeq 1$ .

The zeroes of  $\mathcal{Im} D$  in Eq. (2.2) determines the peaks of resonances. If the summations are neglected, from Eq. (2.3), they occur at  $k\Delta = \pi/2, 3\pi/2$ , etc., which just correspond to resonances inside the corrugation or when the depth  $\Delta$  is an odd number of the quarter wavelength. This term contributes very sharp resonances. Usually only the first one will be visible to the beam because the higher resonances are at very high frequencies. Take the case of a corrugation depth of  $\Delta = 5$  mm,  $\cot k\Delta$  gives resonances at 15, 45, 75, ... GHz. The first summation in  $D$  represents all the above-cutoff modes of waves that can propagate along the beam pipe so that the sharp resonances will be damped heavily. The second summation, which is imaginary, represents all the below-cutoff modes that attenuate along the beam pipe. Its effect can be thought of as fields clinging to the opening of the corrugation, thus making the corrugation depth  $\Delta$  effectively longer and the resonance frequencies smaller. In fact, this is borne out mathematically, since this second summation is positive aside from the factor  $j$ , while  $\cot k\Delta$  is positive for  $k\Delta$  smaller than  $\pi/2$ .

Figure 1 shows the plot of the impedance  $Z_{\parallel}$  due to a corrugation of depth  $\Delta/b = 0.1$  and half width  $g/b = 0.025$ . We see a broad resonance with the resonant frequency shifted from  $kb = \pi b/\Delta = 15.7$  to  $\sim 13$ . This shift is not small at all and is a contribution of all the non-propagating modes. We also see notches located exactly at  $kb = j_{0s}$ , the zeroes of  $J_0$  or the cutoff frequencies of the pipe. These notches are evident from Eq. (2.1), because when  $kb$  approaches  $j_{0s}$  only one term in the summation will contribute. Physically, since  $2g \ll \lambda$ , the wavelength, only the  $z$ -independent mode is favored in the region of the corrugation. At one of the cutoff frequencies, the mode that is just allowed is  $z$ -independent and is therefore favored and dominates over all others. This mode will not penetrate into the corrugation at all and, as a result, the beam does not see the corrugation. We can also say that since this mode is just allowed it has a phase velocity that is infinite and will not interact with the particle beam which has a finite velocity; therefore the coupling impedance  $Z_{\parallel}$  vanishes. The plot also shows some sharp resonances just before the cutoff dips at frequencies below the broad resonance peak. According to Henke, they belong to some well-trapped modes in the region of the cross section enlargement. To us, the physical existence of such trapped modes is not clear at all, because it is hard to see how such small corrugation can trap fields above cutoff. But, mathematically it is clear. The admittance which is proportional to  $D$  has an imaginary part going to infinity at the zeroes of  $J_0$ . For frequencies below the first broad band, as it goes to infinity, it crosses the zero value twice, and, as a result, produces a sharp resonance there. For frequencies above the first broad band and far below the second, the imaginary part of the admittance is always positive; thus no sharp resonances are seen.

For a bellows with many corrugations, the total impedance is not just the sum of the impedances of the individual corrugations. This is because the corrugations are so close together that they interact with each other. However, the situation is not too bad. We expect the notches tend to smooth out because the  $z$ -independent mode is no longer favored. But the overall broad band remains. However, there are other field structures, too; they are mainly due to fields clinging across several corrugations. As a result, the effective depth of the corrugation will be further lengthened and therefore the frequency of the broad band resonance further reduced. It is a good approximation to assume that the position of the broad band and its  $Q$ -value are not altered much; they can therefore be estimated using Eq. (2.2) and possibly Eq. (2.3). The position and quality factor of the broad band  $k_r b$  are then given approximately by

$$\text{Im } D(k_r b) = 0, \quad (2.4)$$

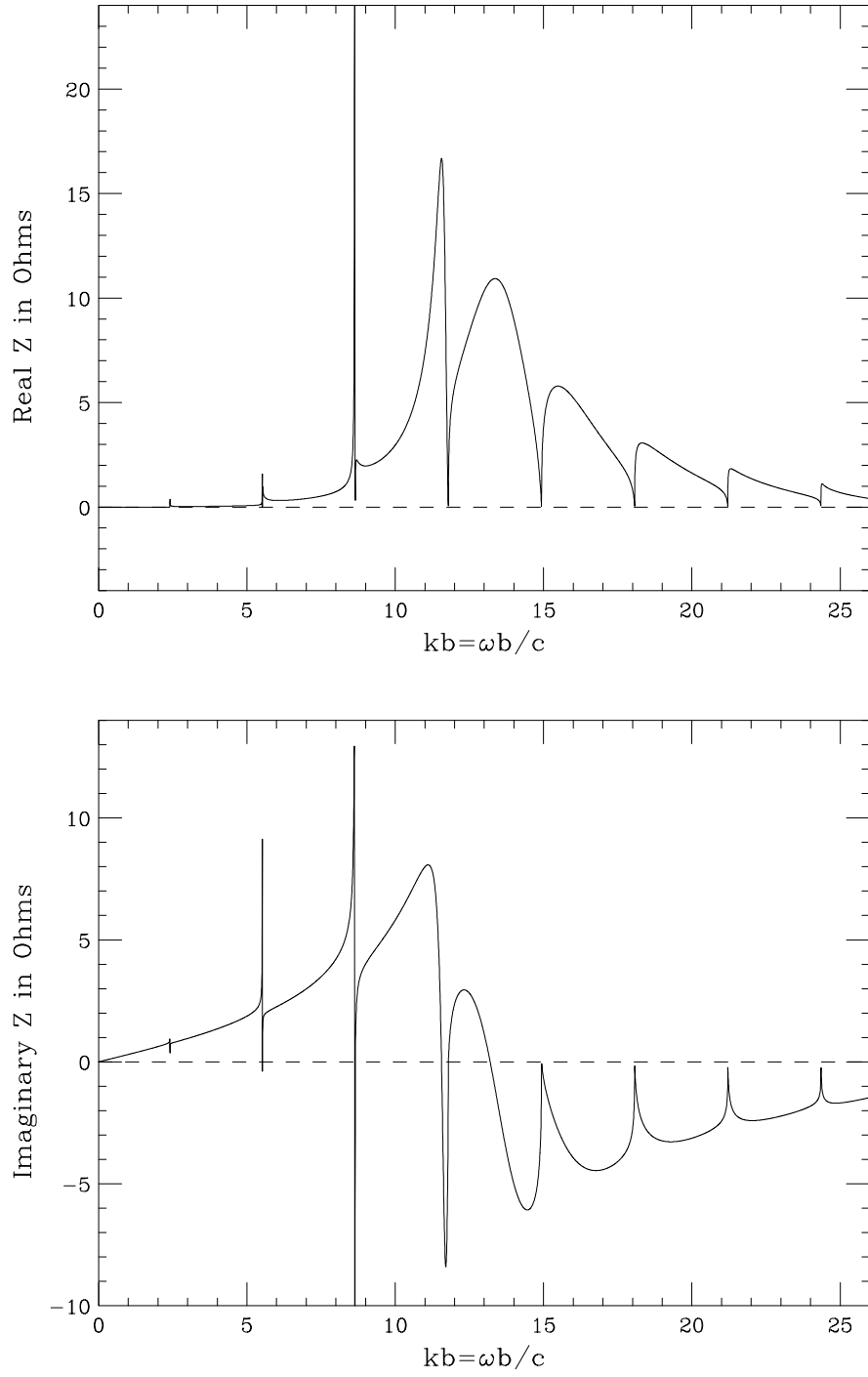


Figure 1: Real and imaginary parts of the longitudinal impedance of one corrugation of a bellows with half width  $g/b = 0.025$  and depth  $\Delta/b = 0.1$  .

$$Q \sim \frac{kb}{2 \operatorname{Re} D} \frac{d \operatorname{Im} D}{d(kb)} \bigg|_{kb=k_r b}. \quad (2.5)$$

The solution of the first equation can only be found numerically. For the examples studied below, the computation of  $Q$  with Eq. (2.5) gives values varying from 3 to 8. We should not expect this formula to be accurate at all due to the notches and sharp peaks that exhibit in the broad band. If one can obtain an simple expression from Eq. (2.1) with the notches and sharp peaks removed, it will serve as an excellent derivation of position,  $Q$  and shunt impedance of the broad band. On the other hand, the extraction of  $Q$  from a TBCI calculation is hardly possible due to truncation of the wake field and noises arising from the finite mesh size. However, for the cases discussed here, the  $Q$ 's do fall between 3 and 8. But this does not imply agreement with Eq. (2.5) in each case. As a whole, it is not a bad idea to assume a rough value of  $Q \sim 5$ .

For a bellows consisting of many corrugations, the standard procedure is to compute the wake function using the code<sup>[1]</sup> TBCI and obtain the impedance via a Fourier transform<sup>[4], [5]</sup>. The code TBCI solves the Maxwell's equations in the time domain and calculate the wake function  $\hat{W}(t)$  of a bunch of unit charge and RMS length  $\sigma_\ell$ ,

$$\hat{W}(t) = \int d\tau q(\tau) W(t - \tau), \quad (2.6)$$

where  $W$  is the wake potential due to a point source and  $q(\tau)$  the charge distribution of the bunch, which is usually taken as a Gaussian truncated at  $\pm 5\sigma_\ell$ . The Fourier transformation of Eq. (2.6) gives  $\hat{Z}(\omega)$ , the effective impedance seen by the bunch, and is related to the actual impedance seen by a point charge  $Z(\omega)$  by

$$\hat{Z}(\omega) = Z(\omega) e^{-\frac{1}{2}(\omega\sigma_\ell/c)^2}. \quad (2.7)$$

Knowing  $\hat{Z}(\omega)$ , the correct  $Z(\omega)$  can be found.

Inner bellows of various sizes are examined. The results are shown in Table 1. The TBCI values are computed with 5 corrugations while the Henke values are for one corrugation using the Eq. (2.4). We see that in each case, the TBCI value is lower. This agrees with our speculation that fields can cling across several corrugations and thus lower resonant frequency. With the exception of Case 11, the agreement is roughly 10%. Case 11 has a corrugation depth of only 0.25 cm, the most shallow among the others. Therefore, the resonant frequency will be very sensitive to the lengthening of the depth by the fields clinging to the opening. Thus, the resonant frequency for five corrugations can differ very much from that of one. Comparing Cases 8, 14 and 15, we learn that the change in resonant frequency  $f_r$  depends very weakly on the corrugation gap  $g$ . A 100% increase in  $g$  lowers  $f_r$  by

Case No.	$b$ cm	$\Delta$ cm	$2g$ cm	$f_r$ in GHz		
				Henke	TBCI( $\parallel$ )	TBCI( $\perp$ )
1	1.50	0.50	0.15	13.3	12.3	12.3
2	2.00	0.50	0.15	12.2	11.5	12.2
3	2.75	0.50	0.15	12.9	11.8	11.6
4	3.25	0.50	0.15	12.2	11.6	11.9
5	3.50	0.50	0.15	13.1	11.7	11.8
6	4.50	0.50	0.15	12.1	11.6	11.8
7	6.15	0.50	0.15	13.1	11.4	11.6
8	6.50	0.50	0.15	12.6	11.4	11.6
9	8.00	0.50	0.15	12.3	11.6	11.3
10	2.00	0.50	0.20	11.9	11.2	11.5
11	2.00	0.25	0.15	24.1	21.0	21.0
12	2.00	0.75	0.15	9.4	8.3	8.3
13	2.00	1.00	0.15	7.4	7.0	7.0
14	6.50	0.50	0.20	12.3	10.8	10.9
15	6.50	0.50	0.30	12.0	10.2	10.3

Table 1: Resonance frequencies of various bellows configurations.

only 9%. If this dependence on  $g$  is neglected, we can obtain a fitted relation shown in Fig. 2,

$$k_r b = 1.37 \left( \frac{\Delta}{b} \right)^{-0.948}, \quad (2.8)$$

where  $k_r = 2\pi f_r/c$ . The fit is a very good one except for Cases 11 and 13. The former may be a result of the shallowness of the corrugation. The latter is the one with  $\Delta/b = 0.5$  which is the biggest of all cases. Thus, we may conclude that Eq. (2.8) gives the correct resonant frequency for  $\Delta/b < 0.5$  and corrugation depth  $\Delta > 0.25$  cm. Similar fit has also been given in Ref. 4 for  $Z_\perp$  using TRANSVRS but the results differ from ours. This empirical formula can also be written as

$$k_r \Delta = 1.37 \left( \frac{\Delta}{b} \right)^{0.052}. \quad (2.9)$$

Since the exponent is small, Eq. (2.9) just says that the fields due to the cutoff modes lower  $k_r \Delta$  from  $\pi/2 = 1.57$  to 1.37.

The transverse impedance of an inner bellows also shows a broad resonance at about roughly the same frequency as the longitudinal impedance. This can easily be understood by considering the bellows corrugation as a radial transmission line.

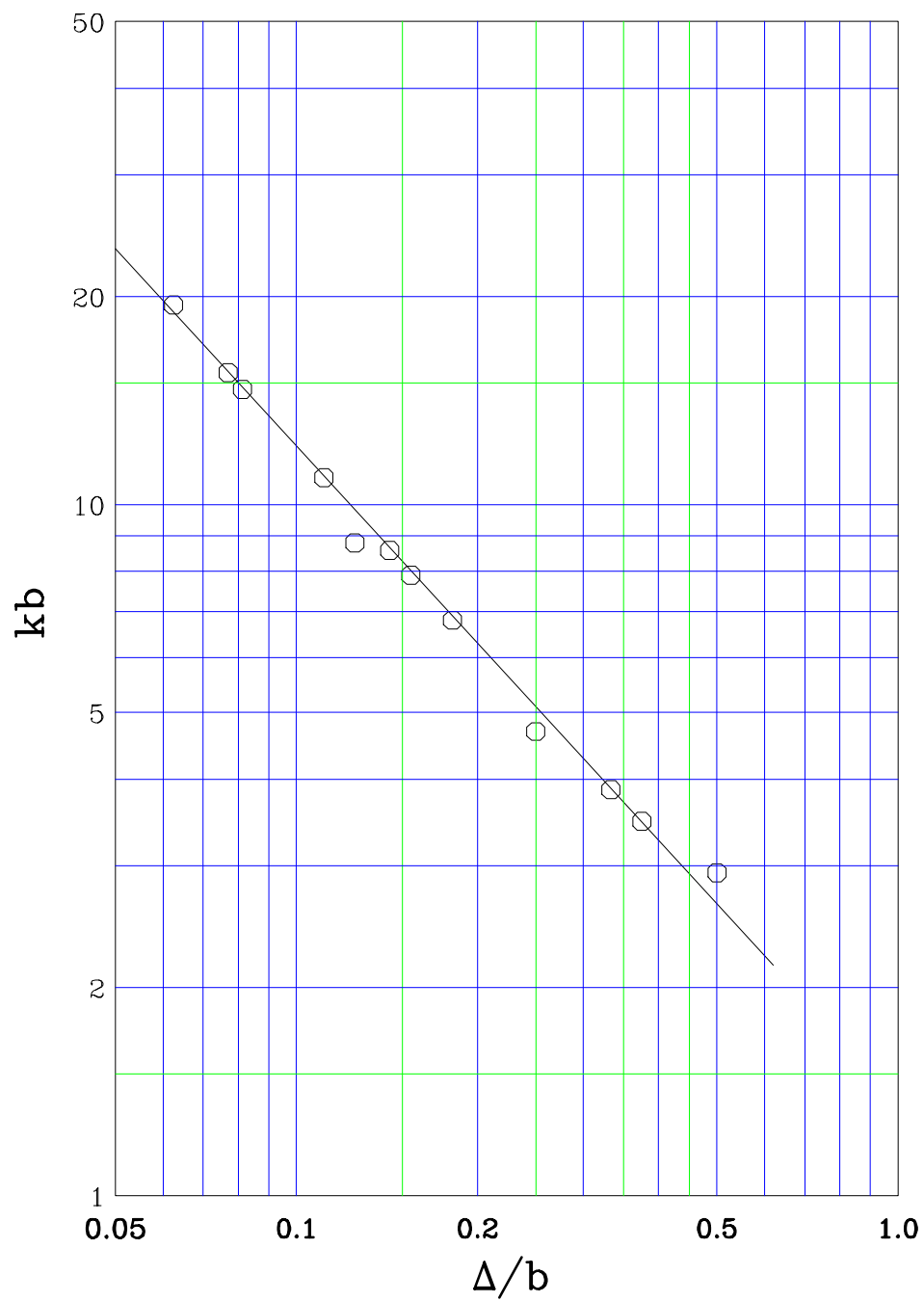


Figure 2: A fit of the resonance position as a function of  $\Delta/b$ .

The resonant frequency is therefore roughly proportional to

$$c \left[ \left( \frac{1}{4\Delta} \right)^2 + \left( \frac{1}{2\pi b} \right)^2 \right]^{1/2}. \quad (2.10)$$

Since  $(2\pi b)^2 \gg (4\Delta)^2$  in most cases, the resonant frequency is dominated by  $\Delta$  only. The resonant frequencies for the above examined cases computed by TBCI are listed in the last column of Table 1. They are, as a whole, the same as those of the longitudinal impedance and can therefore be estimated roughly by solving Eq. (2.4) or read out by the empirical formula of Eq. (2.8) or Eq. (2.9).

### III. LOW FREQUENCY BEHAVIORS

The low frequency behavior of the impedances can be obtained by examining the low frequency magnetic field trapped in the corrugations. When a charged particle passes through a corrugation, electromagnetic fields are left behind. The high-frequency fields are composed of resonances and are usually heavily damped if above cutoff. However, at low frequencies, only azimuthal magnetic field can be trapped as depicted in Fig. 3(a), because the electric field cannot satisfy the required boundary conditions inside the corrugation.

Consider a current of time behavior  $I(t) = I_0 e^{j\omega t}$ . The magnetic flux trapped inside a corrugation or cavity of length  $\ell = 2g$  is

$$\phi_t = \frac{\mu_0 I_0 \ell}{2\pi} \ln \frac{b + \Delta}{b}. \quad (3.1)$$

Only the flux between  $b$  and  $b + \Delta$  has been included because the rest has been taken care of as space-charge contribution. The back e.m.f. induced on the beam is

$$\int E_z dz = -j\omega \phi_t. \quad (3.2)$$

Therefore, the longitudinal impedance per harmonic seen by the beam at low frequencies is<sup>[6]</sup>

$$\frac{Z_{\parallel}}{n} = j \frac{Z_0 \beta \ell}{2\pi R} \ln \frac{b + \Delta}{b}, \quad (3.3)$$

where  $Z_0 = 377 \, \Omega$ ,  $R$  the ring radius, and  $\beta c$  the beam particle velocity.

For the dipole mode, we can make use of the space-charge contribution to the transverse impedance,

$$(Z_{\perp})_{sp} = -j Z_0 R \left( \frac{1}{\beta^2} - 1 \right) \left( \frac{1}{a^2} - \frac{1}{b^2} \right), \quad (3.4)$$

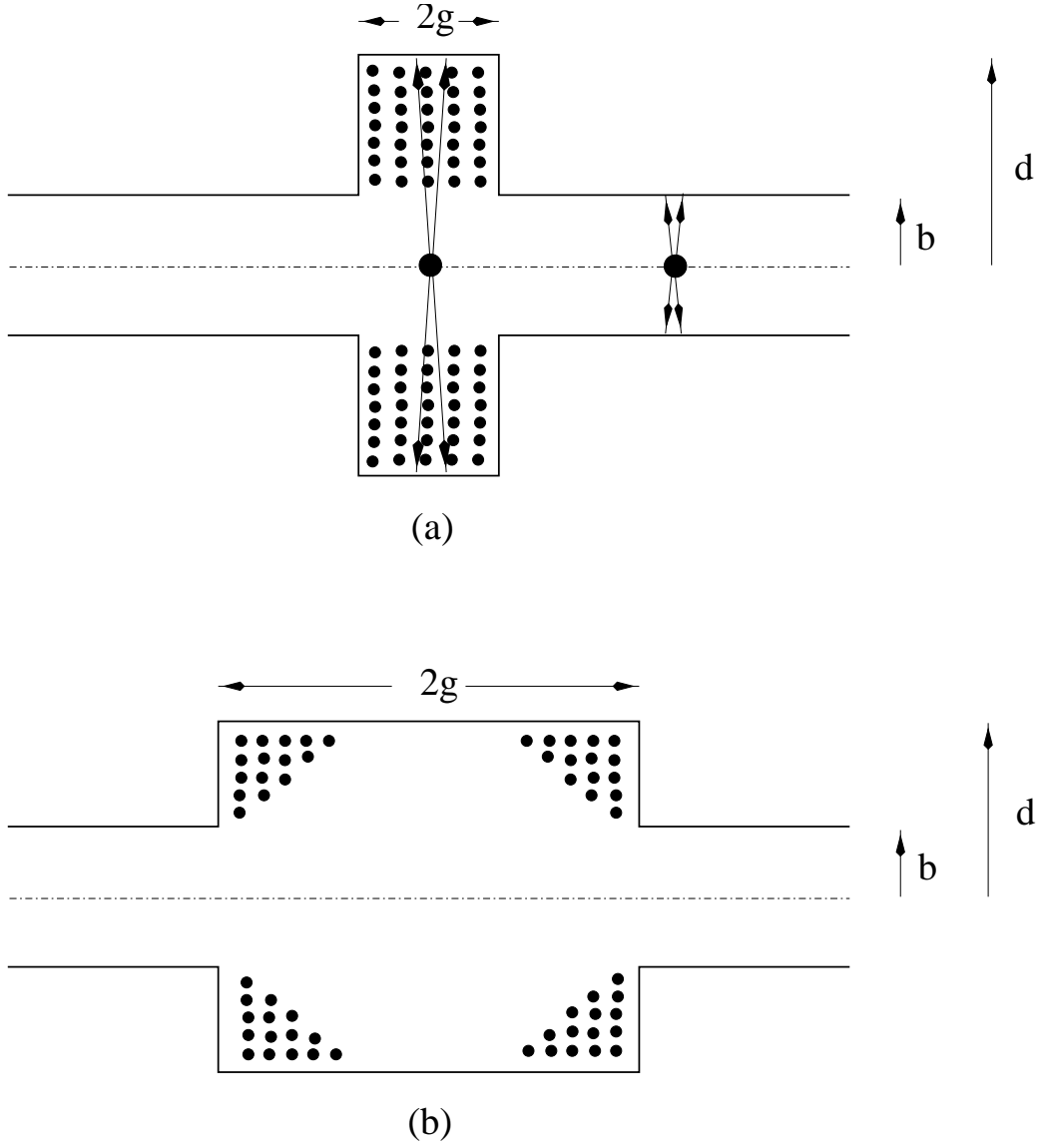


Figure 3: (a) At low frequencies, only azimuthal magnetic flux (dots) can be trapped inside a cavity after the passage of a charged particle whose electric field lines are shown as solid arrows. (b) When the cavity width is much bigger than the step, only the magnetic flux near the corners can be trapped; the flux in the middle leaks away.

where  $a$  is the beam radius. In the first bracket, the first term  $1/\beta^2$  represents the contribution of the electric field while the 1 the contribution of the magnetic field. In the second bracket, the second term  $1/b^2$  is the force due to the image on the beam pipe while the first term  $1/a^2$  is force of the beam on itself. Thus, the contribution of azimuthal magnetic field trapped inside the corrugation can be obtained from Eq. (3.4) by taking only the magnetic part, replacing  $b$  by  $b + \Delta$ , and subtracting away the usual space-charge contribution; or

$$Z_{\perp} = j \frac{Z_0 \ell}{2\pi} \left[ \frac{1}{b^2} - \frac{1}{(b + \Delta)^2} \right]. \quad (3.5)$$

This can be written as

$$Z_{\perp} = j \frac{Z_0 \ell}{\pi b^2} \frac{S^2 - 1}{2S^2}, \quad (3.6)$$

where  $S = (b + \Delta)/b$ . A solution of the Maxwell's equations in the frequency domain<sup>[7]</sup> gives a result,

$$Z_{\perp} = j \frac{Z_0 \ell}{\pi b^2} \frac{S^2 - 1}{S^2 + 1}, \quad (3.7)$$

when  $\ell/b \ll \pi^2/32$ . The difference between the two formulae is not big if  $\Delta/b \ll 1$ . Also in this limit, we find  $Z_{\perp} \propto \Delta/b^3$  while  $Z_{\parallel} \propto \Delta/b$ .

We do not expect Eqs. (3.3) and (3.7) to hold when the length of the cavity is much bigger than the steps or  $\ell \gg 2\Delta$ , because only the magnetic flux near the corners will be trapped and that in the middle will leak away as depicted in Fig. 3(b). In that case,  $\ell$  should be replaced by  $\sim 2\Delta$  in the formulae. Equations. (3.3) and (3.7) can be checked readily by reading out  $\mathcal{I}m Z_{\parallel}/f$  and  $\mathcal{I}m Z_{\perp}$  from the TBCI impedance plots at zero frequency and divided by the number of corrugations. The results are listed in Table 2. We see that the estimation of  $\mathcal{I}m Z_{\parallel}/f$  is excellent, whereas the estimation of  $\mathcal{I}m Z_{\perp}$  seems to be always a bit too high. However, the results of TBCI should not be trusted completely without reservation. In fact TBCI is not sacred. It has been reported<sup>[4]</sup> that TBCI gives different results from the codes<sup>[8], [9]</sup> TRANSVRS and KN7C. Also, for a simple pill-box cavity, a very long transverse wake can lead to unphysical divergent results.

From the single-resonance expressions of impedances in Eqs. (1.1) and (1.2), we get, at zero frequency,

$$\frac{\mathcal{I}m Z_{\parallel}}{f} = \frac{2\pi R_{\parallel}}{\omega_r Q}, \quad (3.8)$$

and

$$\mathcal{I}m Z_{\perp} = \frac{R_{\perp}}{Q}. \quad (3.9)$$

Case	$b$ cm	$\Delta$ cm	$2g$ cm	$\mathcal{Im} Z_{\parallel}/f$ ( $\Omega/\text{GHz}$ )		$\mathcal{Im} Z_{\perp}$ ( $\Omega/\text{m}$ )	
				Eq. (3.3)	TBCI	Eq. (3.7)	TBCI
1	1.50	0.50	0.15	0.542	0.540	224	199
2	2.00	0.50	0.15	0.410	0.410	98.8	89.6
3	2.75	0.50	0.15	0.315	0.310	39.4	36.0
4	3.25	0.50	0.15	0.269	0.270	24.2	22.4
5	3.50	0.50	0.15	0.252	0.256	19.5	18.4
6	4.50	0.50	0.15	0.199	0.202	9.33	8.88
7	6.15	0.50	0.15	0.150	0.147	3.71	3.54
8	6.50	0.50	0.15	0.140	0.140	3.15	3.7
9	8.00	0.50	0.15	0.117	0.117	1.70	1.64
10	2.00	0.50	0.20	0.561	0.556	132	116
11	2.00	0.25	0.15	0.222	0.221	52.8	46.7
12	2.00	0.75	0.15	0.600	0.600	139	124
13	2.00	1.00	0.15	0.764	0.720	173	155
14	6.50	0.50	0.20	0.186	0.190	4.20	3.94
15	6.50	0.50	0.30	0.280	0.277	6.30	5.70

Table 2:  $\mathcal{Im} Z_{\parallel}/f$  and  $\mathcal{Im} Z_{\perp}$  per corrugation at zero frequency.

Thus,  $R_{\perp}/Q$  can be read off from Eq. (3.7) and  $R_{\parallel}/Q$  can be computed using Eq. (3.3) and the resonant frequency  $\omega_r$  determined in Section II.

## IV. ENERGY LOSS

A bunch of longitudinal distribution  $\rho(z - ct)$  will lose energy at the rate of

$$\frac{d\epsilon}{dt} = \frac{c^3}{R} \int_{-\infty}^{\infty} d\omega |\tilde{\rho}(\omega)|^2 Z_{\parallel}(\omega), \quad (4.1)$$

where the bunch spectrum is given by

$$\tilde{\rho}(\omega) = \frac{1}{2\pi c} \int_{-\infty}^{\infty} dz \rho(z) e^{j\omega z/c}, \quad (4.2)$$

and the longitudinal impedance is averaged over  $2\pi R$ , the circumference of the storage ring. For a Gaussian bunch of RMS length  $\sigma_{\ell}$ , the bunch spectrum is

$$\tilde{\rho}(\omega) = \frac{eN}{2\pi c} e^{-\omega^2 \sigma_{\ell}^2 / 2c^2}, \quad (4.3)$$

where  $N$  is the number of particles in the bunch, each carrying charge  $e$ . The rate of loss of energy can then be written as

$$\frac{d\epsilon}{dt} = e^2 N^2 f_0 k_{\parallel}. \quad (4.4)$$

Here,  $f_0$  is the revolution frequency and

$$k_{\parallel} = \frac{1}{\pi} \int_0^{\infty} d\omega e^{-(\omega\sigma_{\ell}/c)^2} \mathcal{Re} Z_{\parallel}(\omega). \quad (4.5)$$

This quantity is sometimes important especially for a superconducting ring.

The energy loss across the bellows is also computed in the TBCI run. However, assuming the impedance expression for one resonance, it can be computed analytically. Substituting Eq. (1.1) into Eq. (4.5) and carrying out the integration, we obtain, for *one* corrugation of the bellow<sup>[10]</sup>,

$$k_{\parallel} = \frac{R_{\parallel}\omega_r}{2Q\alpha} \left(1 - \frac{1}{4Q^2}\right)^{-1/2} \mathcal{Re}[zw(z)]. \quad (4.6)$$

In above,

$$\alpha = \frac{\omega_r\sigma_{\ell}}{c}, \quad (4.7)$$

$$z = \left(\sqrt{1 - \frac{1}{4Q^2}} + \frac{j}{2Q}\right) \alpha, \quad (4.8)$$

and  $w(z)$  is the complex error function.

Let us examine firstly the situation of a very short bunch and a very long bunch. For a very short bunch,  $\alpha \rightarrow 0$ , we have

$$w(z) = 1 + \frac{2j}{\sqrt{\pi}}z - z^2 + O(z^3). \quad (4.9)$$

Thus,

$$k_{\parallel} = \frac{R_{\parallel}\omega_r}{2Q} \left(1 - \frac{2\alpha}{\sqrt{\pi}Q}\right). \quad (4.10)$$

Note that the first term is nothing but the area under one resonance divided by  $\pi$  just as expected from Eq. (4.6) by putting  $\sigma_{\ell} = 0$ .

For the other extreme, when  $\alpha \rightarrow \infty$ , we have

$$w(z) = \frac{j}{\sqrt{\pi}z} + \frac{j}{2\sqrt{\pi}z^3} + O(z^{-5}). \quad (4.11)$$

On substituting into Eq. (4.6), the  $O(z^{-1})$  term in  $w(z)$  does not contribute; the next higher order term gives

$$k_{\parallel} = \frac{R_{\parallel}\omega_r}{4\sqrt{\pi}Q^2\alpha^3}. \quad (4.12)$$

Thus, when the bunch is long or  $\alpha \gg 1$ , the energy loss will be very small. This can also be seen from Eq. (4.6); if the bunch is long enough the exponential factor will drop to a very small value at the resonance of  $Z_{\parallel}$  giving negligible contribution. A general shape of the energy loss  $k_{\parallel}$  versus  $\alpha$  is displayed in Fig. 4.

Take for example the Superconducting Super Collider (SSC) where  $\sigma_{\ell} = 7$  cm. If the corrugations have a depth of 0.5 cm, period 0.30 cm and are of an inner bellows configuration having a beam pipe radius of 1.65 cm, the broad resonance is at  $\sim 12.3$  GHz, according to Eq. (2.9). Using Eqs. (3.5) and (3.8), one gets  $R_{\parallel}/Q = 6.14 \Omega$  for each corrugation. The parameter  $\alpha = \omega_r\sigma_{\ell}/c = 18.0$ , so Eq. (4.12) can be used. The energy loss is therefore  $k_{\parallel} = 1.14 \times 10^7/Q \Omega/\text{sec}$  for one corrugation. In the SSC, there are 1.2 km of bellows or 400,000 corrugations. There are 17,280 bunches each with  $7.3 \times 10^9$  particles. The revolution frequency is 3.614 kHz. Thus, Eq. (4.4) implies an energy loss of  $389/Q$  watts. With a nominal quality factor of  $Q \sim 5$ , this amounts to an energy deposit on the beam pipe at the rate of 78 watts.

For the transverse coupling impedance, there is a similar loss factor defined as

$$k_{\perp} = \frac{1}{2\pi j} \int_{-\infty}^{\infty} d\omega Z_{\perp}(\omega) e^{-(\omega\sigma_{\ell}/c)^2}, \quad (4.13)$$

where a Gaussian bunch has been assumed. Using Eq. (1.2), the integral can be done in the closed form:

$$k_{\perp} = \frac{R_{\perp}\omega_r}{2Q} \left(1 - \frac{1}{4Q^2}\right)^{-1/2} \mathcal{I}m w(z). \quad (4.14)$$

For a very short bunch or  $\alpha \ll 1$ , using Eq. (4.9), we get

$$k_{\perp} = \frac{R_{\perp}\omega_r\alpha}{\sqrt{\pi}Q}, \quad (4.15)$$

which goes to zero when  $\alpha \rightarrow 0$ . This is expected because when the bunch length is exactly zero, the exponential in Eq. (4.13) can be deleted and the transverse impedance when integrated from  $-\infty$  to  $\infty$  vanishes according to Eq. (1.3).

On the other hand, when  $\alpha \gg 1$ , the expansion of Eq. (4.11) gives

$$k_{\perp} = \frac{R_{\perp}\omega_r}{2\sqrt{\pi}Q\alpha}. \quad (4.16)$$

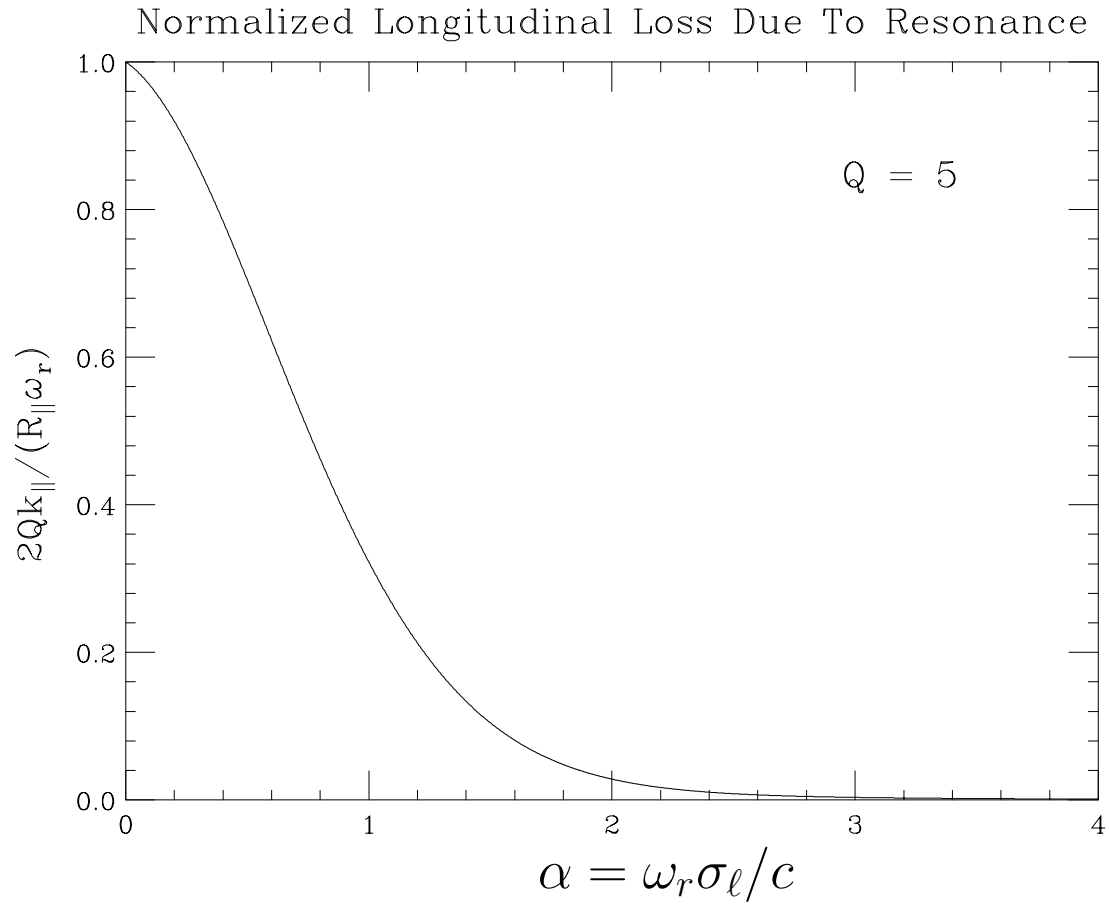


Figure 4: Plot of  $k_{\parallel}$  versus  $\alpha = \omega_r \sigma_\ell / c$ .

This agrees with the direct integration of Eq. (4.13) by letting  $Z_{\perp}(\omega) = Z_{\perp}(0)$  and taking it out of the integration sign.

In fact, when  $Q \gg 1$ ,  $z$  is almost real and is equal to  $\alpha$ . When  $Q \gg \sqrt{\pi}\alpha/2$ , Eq. (4.14) can be rewritten as

$$k_{\perp} = \frac{R_{\perp}\omega_r}{\sqrt{\pi}Q}F(\alpha). \quad (4.17)$$

In above,  $F(\alpha)$  is the Dawson's integral defined as

$$F(\alpha) = e^{-\alpha^2} \int_0^{\alpha} e^{t^2} dt, \quad (4.18)$$

which has a maximum of 0.5410 at  $\alpha = 0.9241$ . The general shape of  $k_{\perp}$  as a function of  $\alpha$  is plotted in Fig. 5.

Both  $k_{\parallel}$  and  $k_{\perp}$  are computed using Eqs. (4.6) and (4.14). The values of  $R_{\parallel}/Q$  and  $R_{\perp}/Q$  are computed from Eqs. (3.3), (3.7), (3.8) and (3.9). The quality factor is assumed to be  $Q = 5$ . The results are compared with those obtained from TBCI and are tabulated in Table 3. The agreement is satisfactory.

Case	$b$ cm	$\Delta$ cm	$2g$ cm	$k_{\parallel}$		$k_{\perp}$	
				Eq. (4.6)	TBCI	Eq. (4.14)	TBCI
1	1.50	0.50	0.15	0.782	0.700	44.6	45.4
2	2.00	0.50	0.15	0.591	0.534	19.9	18.4
3	2.75	0.50	0.15	0.454	0.390	7.86	7.06
4	3.25	0.50	0.15	0.388	0.332	4.87	4.30
5	3.50	0.50	0.15	0.363	0.312	3.92	3.46
6	4.50	0.50	0.15	0.287	0.244	1.86	1.66
7	6.15	0.50	0.15	0.216	0.178	0.73	0.66
8	6.50	0.50	0.15	0.201	0.169	0.62	0.56
9	8.00	0.50	0.15	0.168	0.139	0.33	0.30
10	2.00	0.50	0.20	0.805	0.696	25.6	23.4
11	2.00	0.25	0.15	0.177	0.164	13.1	11.5
12	2.00	0.75	0.15	0.707	0.650	18.8	11.5
13	2.00	1.00	0.15	0.745	0.666	18.4	19.5
14	6.50	0.50	0.20	0.263	0.220	0.78	0.70
15	6.50	0.50	0.30	0.386	0.308	1.10	0.95

Table 3:  $k_{\parallel}$  in  $10^{11}$   $\Omega$ /sec and  $k_{\perp}$  in  $10^{11}$   $\Omega$ /m/sec per corrugation. RMS bunch length is 4 mm and  $Q = 5$ .

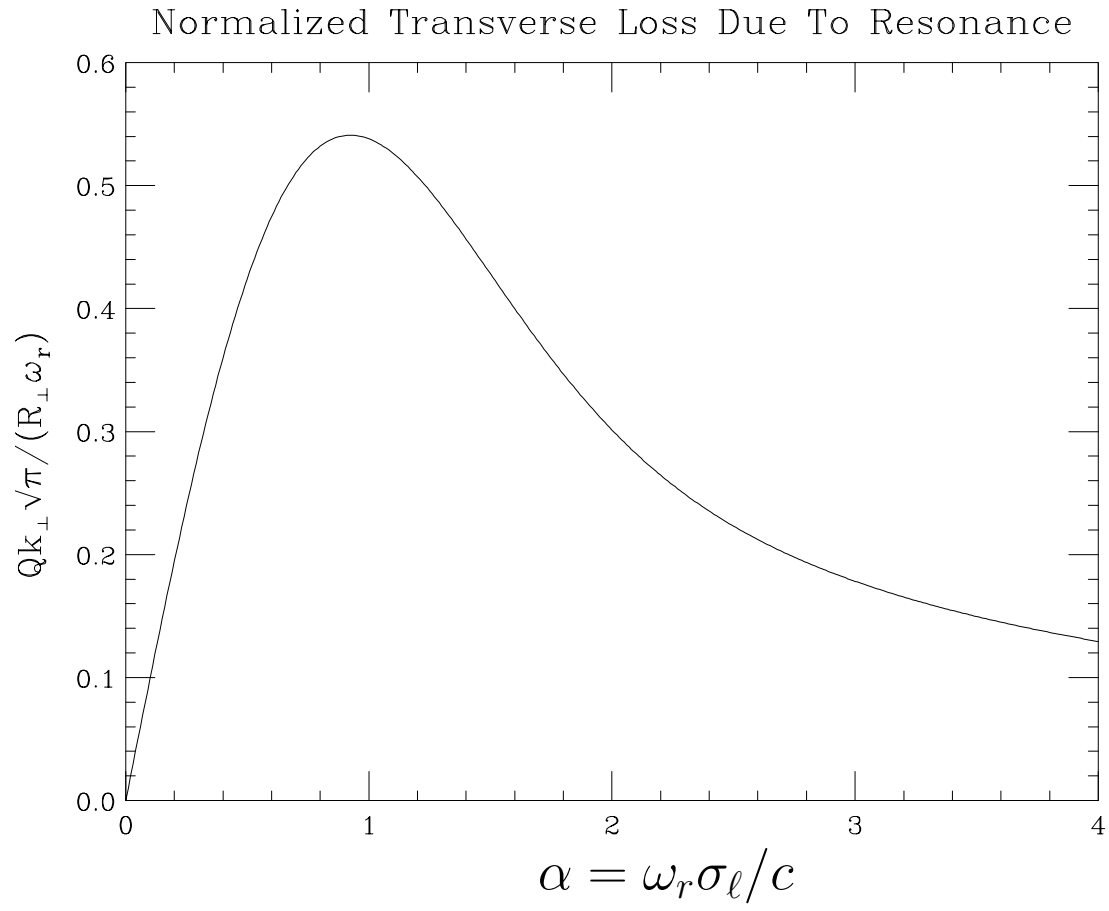


Figure 5: Plot of  $k_\perp$  versus  $\alpha = \omega_r \sigma_\ell / c$ .

## V. THE EFFECTS OF MANY CORRUGATIONS

We have examined the situation of having 1, 5, 20 and 40 corrugations, each of depth  $\Delta = 0.5$  cm, period  $4g = 0.3$  cm. The beam pipe radius is  $b = 2.0$  cm and the RMS bunch length is  $\sigma_\ell = 4$  mm. The TBCI results are listed in Table 4. We see

$n$	$f_{r\parallel}$ GHz	$f_{r\perp}$ GHz	$\mathcal{I}m Z_{\parallel}/f$ $\Omega/\text{GHz}$	$\mathcal{I}m Z_{\perp}$ $\Omega/\text{m}$	$k_{\parallel}$ $10^{11}\Omega/\text{sec}$	$k_{\perp}$ $10^{11}\Omega/\text{m/sec}$
1	12.1	13.2	0.413	85.8	0.561	22.3
5	11.5	12.2	0.410	89.6	0.534	19.9
20	10.0	10.3	0.407	83.4	0.520	16.7
40	9.0	9.7	0.414	86.5	0.530	16.0

Table 4: The resonant frequencies, impedances at zero frequency and loss factors for  $n = 1, 5, 20, 40$  corrugations. All values shown are per corrugation. Each corrugation has a depth of 5 mm and period 3 mm. The beam pipe radius is 2 cm and the RMS bunch length 4 mm.

that resonant frequencies are lowered with more corrugations as we have anticipated. The transverse loss factor  $k_{\perp}$  also decreases with more corrugations. However, it is interesting to see that  $\mathcal{I}m Z_{\parallel}/f$ ,  $\mathcal{I}m Z_{\perp}$  and  $k_{\parallel}$  are almost independent of the number of corrugations. These are in fact the quantities used in the study of single-bunch and coupled-bunch instabilities as well as parasitic heating. In other words, we can safely use the formulae developed in the previous sections to compute these quantities per corrugation, multiply them by the number of corrugations in the ring, and use the final results in the stability criteria and parasitic energy loss formula.

## References

- [1] T. Weiland, DESY Report 82-015 (1982) and Nucl. Inst. and Meth. **212**, 13 (1983).
- [2] CERN Report CERN-LEP-RF/85-41.
- [3] R. L. Gluckstein, private communication.

- [4] K. Bane and R. Ruth, in *Report of the SSC Impedance Workshop*, Lawrence Berkeley Laboratory, Berkeley, June 1985, ed. J. Bisognano, SSC Central Design Group Internal Report No. SSC-SR-1017, p. 10.
- [5] J. Bisognano and K. Y. Ng, *ibid*, p. 45.
- [6] E. Keil and W. Zotter, *Particle Accelerator* **3**, 11 (1972).
- [7] K. Y. Ng, Fermilab Report FN-389.
- [8] K. Bane and B. Zotter, *Proceedings of the 11<sup>th</sup> Int. Conf. on High Energy Accelerators*, CERN (Birkhäuser Verlag, Basel, 1980), p. 580.
- [9] E. Keil, *Nucl. Instr. and Meth.*, **100**, 419 (1972).
- [10] M. Furman, SSC Central Design Group Internal Report SSC-N-142 (1986).